NANO LETTERS

Letter

pubs.acs.org/NanoLett

Efficient Light-Emitting Diodes Based on Nanocrystalline Perovskite in a Dielectric Polymer Matrix

Guangru Li, Zhi-Kuang Tan, Dawei Di, May Ling Lai, Lang Jiang, Jonathan Hua-Wei Lim, Richard H. Friend, and Neil C. Greenham*

Cavendish Laboratory, University of Cambridge, J. J. Thomson Avenue, Cambridge CB3 0HE, United Kingdom

Supporting Information

ABSTRACT: Electroluminescence in light-emitting devices relies on the encounter and radiative recombination of electrons and holes in the emissive layer. In organometal halide perovskite light-emitting diodes, poor film formation creates electrical shunting paths, where injected charge carriers bypass the perovskite emitter, leading to a loss in electroluminescence yield. Here, we report a solution-processing method to block electrical shunts and thereby enhance electroluminescence quantum efficiency in perovskite devices. In this method, a blend of perovskite and a polyimide precursor dielectric (PIP) is solution-deposited to form perovskite nanocrystals in a thin-film matrix of PIP. The PIP forms a pinhole-free charge-blocking layer, while still allowing the embedded perovskite crystals to form electrical contact with the electron- and hole-injection layers. This modified structure reduces nonradiative current losses and improves quantum efficiency by 2 orders of magnitude, giving an external quantum efficiency of 1.2%. This simple technique provides an alternative route to circumvent film formation problems in perovskite optoelectronics and offers the possibility of flexible and high-performance light-emitting displays.

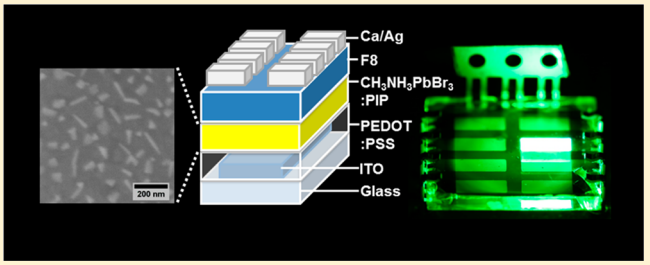

KEYWORDS: *Perovskite light-emitting diode, perovskite-polymer blend, perovskite nanocrystals, perovskite morphology*

Solution processing of luminescent semiconductors presents a particularly attractive option for the low-cost fabrication of light-emitting devices.[1−4] Recent work on high-efficiency organometal halide perovskite photovoltaics has shown these materials to possess both the remarkable qualities of traditional semiconductors and the facile processability of organic semiconductors.[5−9] A new report on perovskite nanoparticles has further shown these materials to possess high photoluminescence quantum yield.[10] The perovskite materials also benefit from low cost and earth-abundance and can be deposited at low temperatures under ambient conditions. More recently, bright and color-controlled electroluminescence was reported in perovskite light-emitting diodes (PeLEDs), thereby opening up a potential range of display and lighting applications for these materials.[11,12] However, the quantum efficiencies in these PeLED devices remain modest due to difficulties in the formation of uniform thin films.

Light emission occurs when injected electrons and holes meet in the perovskite layer and recombine radiatively. However, it is easy for injected charges to bypass the perovskite layer through pinholes in the thin films, leading to nonradiative current losses and a lower efficiency. Difficulties in the formation of uniform and pinhole-free perovskite films are well known, due to the crystalline nature of the material. This problem is further exacerbated by the sublimation of excess methylammonium halide precursor during thermal annealing, thereby leaving voids in the perovskite layer. New techniques involving sequential or vapor deposition of perovskite precursors have been developed to improve film formation in the thick perovskite layers used for photovoltaics,[7,13] but these techniques do not completely eliminate pin-holes and hence are not a sufficient solution for the ultrathin (<50 nm) layers[11] required for light-emitting devices.

In this Letter, we report the fabrication of efficient light-emitting diodes through the embedding of perovskite nanocrystals in a thin matrix of dielectric polymer. The perovskite nanocrystals form in situ when a blend of perovskite precursor and polymer is deposited and annealed. The uniformly distributed perovskite nanocrystals provide good light emission, while the dielectric polymer fills in the surrounding voids to block nonradiative current losses.

Our devices use the poly(9,9-dioctylfluorene) (F8) as an electron-transporting layer, which blocks injected holes from leaving the device, and also serves as a spacer layer to prevent luminescence quenching at the metal electrode.[11] In addition, the semiconducting F8 forms a good conformal coating and prevents the top electrode from shorting through the thin (<50 nm) perovskite layer. The low-workfunction calcium electrode provides ohmic electron injection, while the high-workfunction poly(3,4-ethylenedioxythiophene):poly(styrenesulfonate) (PEDOT:PSS) acts as the hole-injection layer.

Received: January 20, 2015
Published: February 24, 2015

DOI: 10.1021/acs.nanolett.5b00235
Nano Lett. 2015, 15, 2640−2644

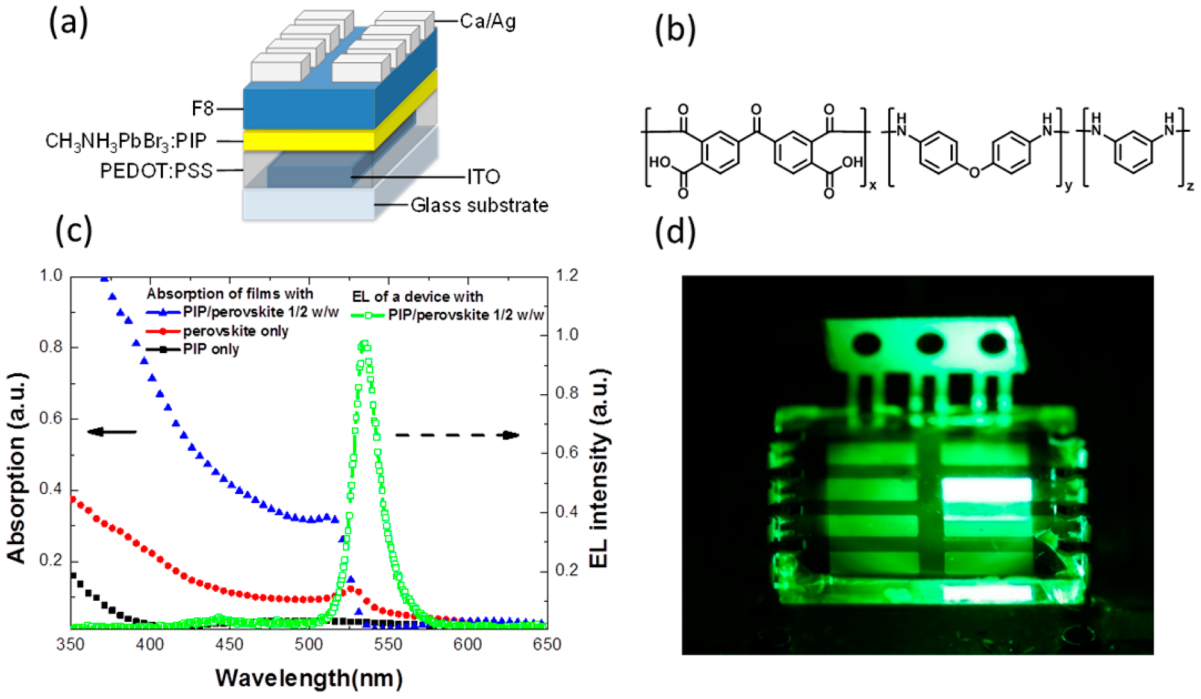

Figure 1. (a) Device structure of a $CH_3NH_3PbBr_3$ PeLED. (b) Chemical structure of PIP polymer (product number PI2525, purchased from HD microsystems) (c) Absorption spectra of PIP, $CH_3NH_3PbBr_3$ and blend films, and electroluminescence spectrum (dashed line) of a $CH_3NH_3PbBr_3$/PIP PeLED. (d) Image of light emission from the second pixel on the right side of a $CH_3NH_3PbBr_3$/PIP PeLED. The dimmer light below the illuminated pixel originates from multiple internal reflections within the glass substrate.

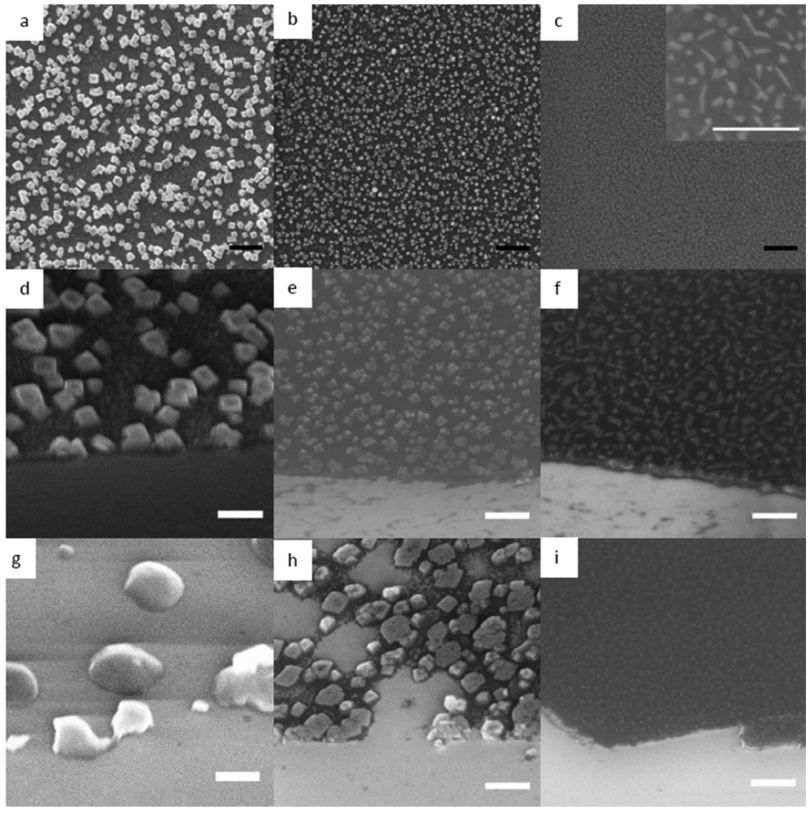

Figure 2. Top view SEM image of (a) perovskite only, (b) 1/10 PIP/perovskite, and (c) 1/2 PIP/perovskite on PEDOT:PSS coated silicon. Inset in (c) shows an enlarged image of 1/2 PIP/perovskite film. (d–f) Panels show 45° angled view of (a–c), respectively. (g–i) Panels show a 45° angled view of films spin-coated with the same solution as in (a–c) but on bare silicon substrates. All black scale bars represent 1 μm. All white scale bars represent 500 nm.

DOI: 10.1021/acs.nanolett.5b00235
Nano Lett. 2015, 15, 2640–2644

The structure of our devices is ITO/PEDOT:PSS/Perovskite−PIP/F8/Ca/Ag, as shown in Figure 1a. We use a large-bandgap perovskite, $CH_3NH_3PbBr_3$, as a green emitter layer. The perovskite precursors are made by blending CH_3NH_3Br and $PbBr_2$ at 5 wt % in *N*,*N*-dimethylformamide (DMF) at a molar ratio of 3:2. A commercial aromatic polyimide precursor (PIP) dissolved in *N*-methyl-2-pyrrolidone (NMP) is blended with perovskite precursor solutions in different weight ratios. The chemical structure of PIP is shown in Figure 1b. This polymer was chosen because it can associate well with the hybrid perovskite and can be readily processed in DMF, possibly due to its polar functional group and hydrophilicity.[14] The polymer is also transparent and electrically insulating and therefore suitable for use as a charge-blocking material in a light-emitting device. The use of a polymer in the composite layer also potentially offers the benefit of enhanced material stability, as previously demonstrated in 2D-perovskite-polymer mixtures.[15,16] The perovskite nanocrystal−PIP polymer composite forms upon spin-coating the blend solutions on PEDOT:PSS and annealing the resulting films at 60 °C for 1 min. We note that the PIP polymer remains in its unimidized precursor form under our processing conditions, because a temperature of 200 °C is typically required for imidization ring-closure to take place.[17] The formation of perovskite crystals in the presence of a polymer matrix is confirmed by X-ray diffraction studies (Supporting Information Figure S1).

Figure 1c shows the absorption spectrum of the perovskite/PIP film and its electroluminescence in a device structure. The PeLEDs display a strong green electroluminescence at 534 nm with a narrow full width at half-maximum (fwhm) of 19 nm. There is negligible absorption of the green perovskite emission by the PIP polymer. As shown in Figure 1d, electroluminescence from a representative device is uniform across the entire device pixel with no sign of large-scale inhomogeneity, demonstrating that the emission from perovskite nanocrystals is uniformly distributed across the spin-coated film.

We studied the morphology of the composite layer with various perovskite to PIP ratios, using scanning electron microscopy (SEM). Figure 2a−c shows top-view SEM images of perovskite-only, PIP−perovskite 1:10 w/w ratio and 1:2 w/w ratio films, respectively, deposited on top of a PEDOT:PSS coated silicon substrate. Figure 2d−f shows the corresponding SEM images of the scratched edge of each film, taken at an angle of 45°. The brighter areas represent perovskite because they have a higher electron density than the surrounding polymer. The films in Figure 2a−f were deposited on PEDOT:PSS in order to ensure that the images are representative of the perovskite layers in the PeLED structures.

As shown in Figure 2a,d, the perovskite-only "layer" consists of cuboid nanocrystals of approximately 250 nm in dimension, and they occupy 33% of the layer area. In the 1:10 ratio film as shown in Figure 2b,e, the addition of PIP causes the nanocrystal sizes to decrease to 100 nm, and the perovskite nanocrystals occupy approximately 27% of the film area. The nanocrystals shrink further to just 60 nm in the 1:2 ratio film and occupy 28% of the area, as shown in Figure 2c,f.

From the 45° SEM images (Figure 2d−f), which show the scratched edges of the films, we can see that the perovskite crystals are embedded in a uniform layer of polymer. The light area shows the bare silicon substrate where the film has been removed, the darker area shows the polymer layer, and the lighter cuboidal and polyhedronal objects within the polymer represent embedded perovskite crystals. Because it is difficult to discriminate between PEDOT:PSS and PIP in these images, we also took 45° SEM images of perovskite films that are deposited on bare silicon substrates, as shown in Figure 2g−i. The different substrate produces some changes in the perovskite crystal morphology, as expected due to different wetting properties. While in the 1:10 ratio film (Figure 2h) the PIP polymer layer is incomplete in certain areas, the 1:2 ratio film in Figure 2i shows complete PIP polymer coverage with no signs of pinholes.

Through these SEM results, we can deduce that the perovskite nanocrystals form within a matrix of dielectric PIP in the blend films. As shown in the atomic force microscopy (AFM) measurements in Supporting Information Figure S2, the thickness of the PIP polymer was determined to be 7 and 30 nm in the 1:10 and 1:2 weight ratio films, respectively, and the average thicknesses of the entire PIP−perovskite composite films are 11, 25, and 33 nm for the perovskite-only, 1:10, and 1:2 weight ratio films.

We tested the performance of the above composite films in a light-emitting diode structure. Figure 3a shows the luminance and current density versus voltage characteristics of devices with PIP−perovskite weight ratios of 1:10, 1:2 and 1:1 as well as a control device with only perovskite in the emissive layer (no PIP added). Through the increase in the blending ratio of PIP, the current density is reduced at each driving voltage and the luminance is enhanced, thereby leading to a dramatic enhancement in device efficiency. For instance, in the 1:2 ratio device a current density of 3.1 mA cm^{-2} is required to produce a luminance of 200 cd m^{-2}, but much larger current densities of 580 and 57 mA cm^{-2} are required for the perovskite-only and the 1:10 ratio devices, respectively, to achieve the same luminance. Figure 3b shows the corresponding external quantum efficiency (EQE) of the respective devices. With the addition of PIP, the devices show a clear increase in quantum efficiency. In particular, the EQE increased by more than 2 orders of magnitude from 0.01% in devices without PIP to 1.2% in devices with a 1:1 PIP to perovskite ratio.

We further investigated the PIP−perovskite composite LEDs over a wider range of mixing ratios and plotted their device performance in Figure 3c. The best peak EQE of ∼1% is achieved between a 1:2 and 1:1 PIP to perovskite ratio. This represents a 10-fold enhancement of device efficiency over the previous report.[11,12] At higher ratios, the device efficiency drops and the variance in device performance increases. Some devices that contained large polymer fractions were too resistive and failed to work. We show in Supporting Information Figure S3 that PIP-only devices were completely insulating.

These device studies and the SEM characterizations suggest that the 1:2 ratio film provides optimal PIP coverage and effectively blocks pinholes or electrical shunting paths. This leads to low current losses and a significantly enhanced device efficiency. The polymer coverage in the 1:10 ratio films is thinner and possibly incomplete in some areas and therefore provides less protection against current losses. Because the perovskite and PIP composite devices emit efficiently and uniformly up to a 1:1 blend ratio, it is reasonable to assume that the perovskite nanocrystals extend across the thickness of these films, forming electrical contact with both the PEDOT:PSS and the F8 layers.

We further investigated the effects of PIP addition on the electroluminescence spectra of the PeLEDs. As shown in Figure 4, an F8 contribution to electroluminescence could be observed

DOI: 10.1021/acs.nanolett.5b00235
Nano Lett. 2015, 15, 2640−2644

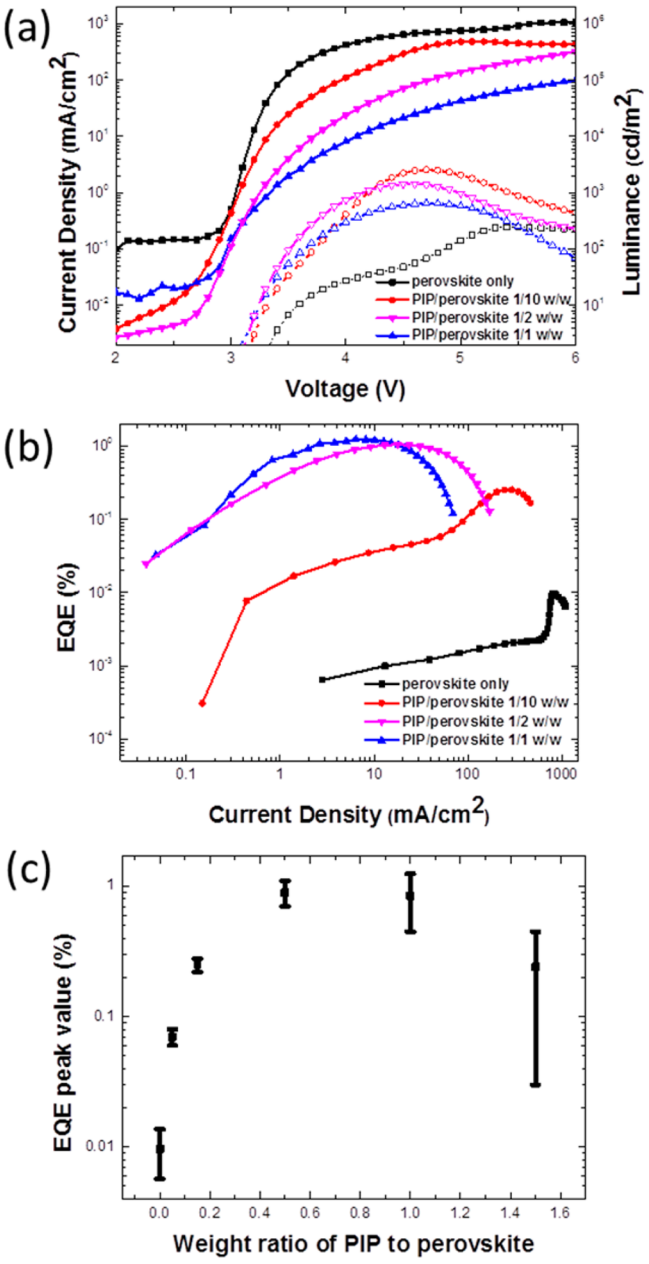

Figure 3. (a) Current density (solid line) versus voltage and luminance (dashed line) versus voltage characteristics of PeLEDs. (b) External quantum efficiency versus current density characteristics of PeLEDs. (c) External quantum efficiency peak value versus $CH_3NH_3PbBr_3$/PIP weight ratio.

between 400 and 500 nm for the perovskite-only devices (no PIP). This F8 emission most likely arises from hole injection directly from PEDOT:PSS into the F8. In contrast, F8 electroluminescence was effectively shut off in the PIP–perovskite PeLEDs and clean perovskite emission was obtained, consistent with suppression of hole injection into the F8. Combined with the improvement in efficiency, this demonstrates that the PIP is remarkably effective in preventing contact between F8 and PEDOT:PSS.

We have shown that luminescent perovskite nanocrystals can be embedded in a pinhole-free matrix of dielectric polymer to give superior light-emitting diode performance. In addition to the benefits associated with solution-processability, the incorporation of an otherwise brittle perovskite material in a

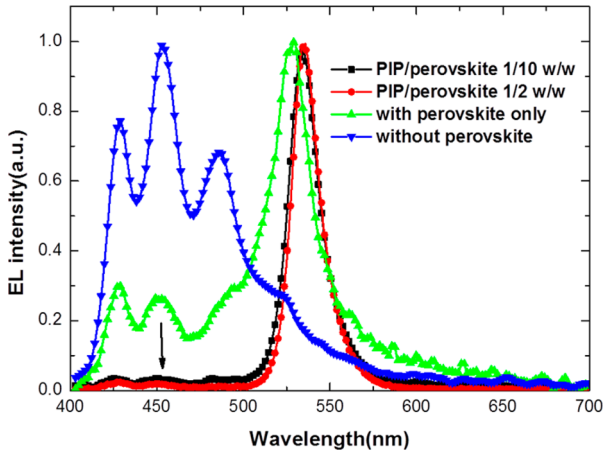

Figure 4. EL spectra of F8 LED, perovskite-only, and PIP/perovskite blend LEDs. All spectra were taken at 5 V bias.

polymer matrix may provide additional benefits of flexibility. It is interesting and perhaps surprising that perovskite crystallites can form and retain their attractive optoelectronic properties within an organic matrix without the need for explicit control or modification of the crystallite surfaces. If it can be extended to thicker layers while maintaining percolation through the nanocrystals, the approach demonstrated here may have benefits in improving film formation in solution-processed perovskite solar cells to reduce shunt resistance problems.

■ ASSOCIATED CONTENT

Supporting Information

Details of the material preparation, PeLED fabrication, and characterization are given. This material is available free of charge via the Internet at http://pubs.acs.org.

■ AUTHOR INFORMATION

Corresponding Author

*E-mail: ncg11@cam.ac.uk.

Author Contributions

The manuscript was written through contributions of all authors. All authors have given approval to the final version of the manuscript.

Notes

The authors declare no competing financial interest.

■ ACKNOWLEDGMENTS

The authors acknowledge funding from the Gates Cambridge Trust, the Singapore National Research Foundation (Energy Innovation Programme Office), the KACST-Cambridge University Joint Centre of Excellence, the Royal Society/Sino-British Fellowship Trust, and the Engineering and Physical Sciences Research Council, UK. We also thank Dr. Alessandro Sepe for helpful discussions of the XRD data.

■ REFERENCES

(1) Burroughes, J. H.; Bradley, D. D. C.; Brown, A. R.; Marks, R. N.; Mackay, K.; Friend, R. H.; Burns, P. L.; Holmes, A. B. *Nature* **1990**, *347*, 539–541.

(2) Greenham, N. C.; Moratti, S. C.; Bradley, D. D. C.; Friend, R. H.; Holmes, A. B. *Nature* **1993**, *365*, 628–630.

(3) Colvin, V. L.; Schlamp, M. C.; Alivisatos, A. P. *Nature* **1994**, *370*, 354–357.

DOI: 10.1021/acs.nanolett.5b00235
Nano Lett. 2015, 15, 2640–2644

(4) Coe, S.; Woo, W.-K.; Bawendi, M.; Bulović, V. *Nature* **2002**, *420*, 800−803.
(5) Lee, M. M.; Teuscher, J.; Miyasaka, T.; Murakami, T. N.; Snaith, H. J. *Science* **2012**, *338*, 643−647.
(6) Burschka, J.; Pellet, N.; Moon, S.-J.; Humphry-Baker, R.; Gao, P.; Nazeeruddin, M. K.; Grätzel, M. *Nature* **2013**, *499*, 316−319.
(7) Liu, M.; Johnston, M. B.; Snaith, H. J. *Nature* **2013**, *501*, 395−398.
(8) Stranks, S. D.; Eperon, G. E.; Grancini, G.; Menelaou, C.; Alcocer, M. J. P.; Leijtens, T.; Herz, L. M.; Petrozza, A.; Snaith, H. J. *Science* **2013**, *342*, 341−344.
(9) Ball, J. M.; Lee, M. M.; Hey, A.; Snaith, H. J. *Energy Environ. Sci.* **2013**, *6*, 1739−1743.
(10) Schmidt, L. C.; Pertegás, A.; González-Carrero, S.; Malinkiewicz, O.; Agouram, S.; Espallargas, G. M.; Bolink, H. J.; Galian, R. E.; Pérez-Prieto, J. *J. Am. Chem. Soc.* **2014**, *136*, 850−853.
(11) Tan, Z.-K.; Moghaddam, R. S.; Lai, M. L.; Docampo, P.; Higler, R.; Deschler, F.; Price, M.; Sadhanala, A.; Pazos, L. M.; Credgington, D.; Hanusch, F.; Bein, T.; Snaith, H. J.; Friend, R. H. *Nat. Nanotechnol.* **2014**, *9*, 687−692.
(12) Kim, Y.-H.; Cho, H.; Heo, J. H.; Kim, T.-S.; Myoung, N.; Lee, C.-L.; Im, S. H.; Lee, T.-W. *Adv. Mater.* **2014**, *27*, 1248−1254.
(13) Chen, Q.; Zhou, H.; Hong, Z.; Luo, S.; Duan, H.-S.; Wang, H.-H.; Liu, Y.; Li, G.; Yang, Y. *J. Am. Chem. Soc.* **2014**, *136*, 622−625.
(14) Salim, T.; Sun, S.; Abe, Y.; Krishna, A.; Grimsdale, A. C.; Lam, Y. M. *J. Mater. Chem. A* **2015**, DOI: 10.1039/C4TA05226A.
(15) Kitazawa, N. *J. Mater. Sci.* **1998**, *33*, 1441−1444.
(16) Wei, Y.; Lauret, J. S.; Galmiche, L.; Audebert, P.; Deleporte, E. *Opt. Express* **2012**, *20*, 10399−10405.
(17) Minges, M. L. Electronic Materials Handbook: Packaging; ASM international: Materials Park, OH, 1989; Vol. *1*.

DOI: 10.1021/acs.nanolett.5b00235
Nano Lett. 2015, 15, 2640−2644